Metamaterial Based High Isolated Four Port MIMO Antenna for 5G Smartphone Applications.

Mohamed S. Alshulle[1*], Areej. M. Ahmeid[2], Hana. R. Matouq[3]

[1]Military Industries Organization, Bani-walid, Libya.

[2,3]College of Electronic Technology, Bani-walid, Libya.

*Crosspnding author: dr.engineeralshole@gmail.com

Abstract: The growth of mobile communications has considerably expanded the number of linked devices. Lack of efficient and small antenna components is one of the most frequent causes of this. The demand for more effective and efficient mobile terminals has substantially risen as a result of the growing number of linked devices and the requirement for high-speed wireless communication. A conventional Multiple Input Multiple Output MIMO antenna system only functions as an antenna array if the coupling between the components is high. However, it is well recognized that this technology has a flaw, and that flaw is the coupling between the various components of the system. In the event that there is a strong connection between the radiating elements, a MIMO antenna system just functions as an antenna array. Because of this, To take use of MIMO technology's advantages, there needs be a significant decoupling between the radiating parts. This paper's major goal is to research and construct printed multi-port MIMO antenna designs with integrated decoupling strategies for 5G smartphones. The excellent electromagnetic characteristics of these materials have drawn a considerable deal of interest in recent years. These substances are man-made structures that display traits not seen in nature. By regularly merging artificial structures, a metamaterial may be created. Additionally possessing lending qualities, metamaterials are known to enhance antenna gain and high isolation coupling when put next to them.

The findings from simulation and measurement are well-coordinated. The suggested structure would work with mm-wave 5G applications in the 28 GHz frequency region. Additionally, the operational frequency band's max gain is 9.14 dB. Metrics of MIMO performance such the Envelope Correlation Coefficient (ECC), Mean Effective Gain (MEG), and Channel Capacity Loss (CCL), Analysis of the suggested structure's diversity gain (DG) The final design incorporated a size/performance trade-off in favor of shrinking the structure's size to enable its application in smaller size devices. and the outcomes show that the design is suitable as a possible competitor for MIMO 5G Smartphone applications. Using Ansoft HFSS, the suggested antennas' simulation was performed.

Keywords: (Multiple Input Multiple Output (MIMO), Voltage Standing Wave Ratio (VSWR), Return Loss (S))

Introduction

RFID technology offers wireless communication. The shift from 4G to 5G technology is now taking place in the realm of mobile communication technology. Users' needs for better wireless communication services are being driven by the fast increase of mobile data. Information must be accessible promptly and quickly, transmission efficiency must be increased, and system security must be improved. As a result, 4G is gradually beginning to fall short of the increased communication requirements, and its flaws are becoming more apparent. From 2020, When 5G reached the commercial stage, it indicated that it was progressively taking over as the standard mobile communication technology. Its frequency range includes the mm-Wave band (24.25-54.6 GHz) and sub-6 GHz (450 MHz-6 GHz). High-speed data transfer and dependable connectivity with minimal latency are the key characteristics of 5G [1]. Furthermore, the 5G user's positive Quality of Experience (QoE) are necessitates superior antenna diversity and increased channel capacity.

Diversity systems with two receivers were created as a solution to multipath effects' signal fading, and thus marked the beginning of the development of MIMO. Studies already conducted [4,5] have demonstrated that, in comparison to simple input simple output (SISO) systems with a straightforward layout as illustrated in Figure (1), MIMO systems include several extra pathways, and by reducing multipath impact, latency, and packet loss, the communication modes may be improved. Additionally, Shannon's theorem states that the signal-to-noise ratio (SNR) and channel bandwidth affect the channel capacity. Additionally, because to the multi-port architecture, MIMO systems have shown the ability to double data throughput with a fixed bandwidth and transmission power [2]. As a result, researching MIMO systems is crucial to creating 5G communication systems.
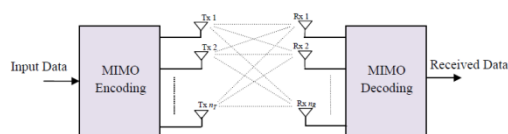

Fig. 1. Block diagram of MIMO wireless system.

One of the greatest electromagnetic revolutions of the 20th century has been predicted by the emergence of metamaterials. Human-made composite materials known as metamaterials enable the customization of electromagnetic and acoustic wave propagation through media. The geometrical arrangement of its constituent parts, sometimes referred to as "meta-atoms," controls a significant portion of the mechanical or electrical response of these artificial structures, much like crystals and protein chains. The most remarkable feature of met materials is their ability to be created with unusual properties that are rarely seen in nature [2], such as artificial magnetism (magnetism without naturally magnetic materials), negative-refractive indices from positive-index materials, and invisibility cloaking (or "invisible" materials that do not interact with light).

As a result, the design difficulties and characteristics for obtaining high channel capacity with minimal complexity pique the interest of the researchers and serve as a motivator for the study and design of multiport MIMO antennas using met-materials for high data rate 5G applications.

This study describes a compact four antenna system for wireless multi-port MIMO applications. Each of the six antennas in the proposed MIMO antenna works at 28 GHz. Each antenna element is created using a single composite right/left unit cell. A novel strategy relies on current cancellation between the antennas to reduce mutual coupling without the use of extra structures. The suggested antenna has

been evaluated for its high isolation, compact size, low cost, and characteristic evaluations of the prototype antenna array's return loss (RL), bandwidth, isolation, VSWR, and radiation pattern.

1. Metamaterials

Because the wave vector, electric-field, and magnetic-field vectors constitute an LH system, metamaterials are often referred to as DNG or LH media. This name was originally used by Veselagoin 1968 [3]. Veselago noted that LH metamaterials (LHMs) exhibit certain unusual features, including the inverse Snell effect, an inverse Doppler shift, and backward-directed Cherenkov radiation in his groundbreaking study [3]. LHMs also have simultaneous negative permittivity and permeability. However, because there weren't any resources that could be used to make his idea until 1999. essential features of In the next subsections, LHMs are described and contrasted with those of conventional materials.

Metamaterials (MTMs) are substances that have been designed to generate electromagnetic characteristics that are rare or challenging to get in nature. Due to their assurance that they will provide permittivity ε, permeability μ and index of refraction, The potential use of metamaterials in several electromagnetic applications has sparked widespread attention. owing to their special electromagnetic characteristics, which include zero propagation constant at non-zero frequency, anti-parallel phase and group velocities, and so on.

The idea that materials with simultaneously negative permittivity and permeability are technically possible and have a negative index of refraction was put up by Russian scientist Victor Georgievich Veselago in the 1960s. These media were given the label "left-handed" by Veselago because they produce a left-handed triplet rather than the right-handed triplet that is produced by traditional right-handed media (RHM) [3].
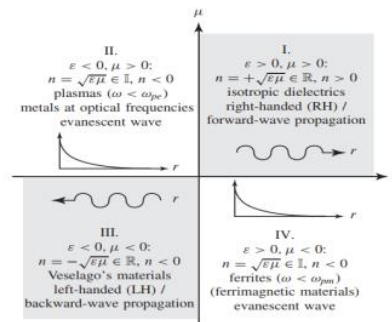

Fig. 2. The possible combinations of permittivity and permeability, [32].

The characteristics of the materials involved affect how a system reacts to the presence of an electromagnetic field. By describing these materials' macroscopic qualities like permittivity and permeability, these properties are characterized. using permeability and permittivity.

2. Design of a CRLH Unit-Cell (Interdigital) Antenna

We take into consideration the unit cell depicted in Figure (3.4) in order to extract the parameters L_R C_R L_L and C_L in the CRLH implementation of Figure (3).Figure (3) (a) depicts the equivalent circuit of this unit cell, which is made up of a series connection between the interdigital capacitor and the shorted stub inductor, while Figure (4) (b) depicts an additional T-network that will be utilized for extraction. The interdigital capacitor's and the stub inductor's scattering parameters are first calculated independently using either measurement or full-wave modeling. To do this, a brief piece of

microstrip TL must be inserted at each end of the component to guarantee the extinction of the higher-order modes caused by the discontinuity in the transition from the coaxial connection to the microstrip. because phase is connected to the most significant characteristics of MTMs. [4].
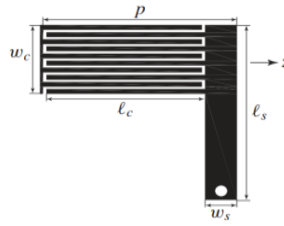

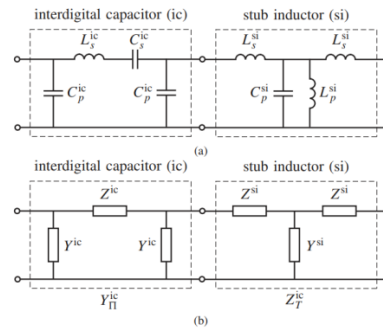**Fig. 3. Unit cell of the microstrip CRLH TL.**

Fig. 4. Circuit models for the parameters extraction of the unit cell. (a) Equivalent circuit. (b) Auxiliary equivalent π and T networks.

the calculations for the ZOR antenna design's original unit cell model. The arrangement was changed several times to get the desired outcome, as illustrated in Figures (5) and (6).
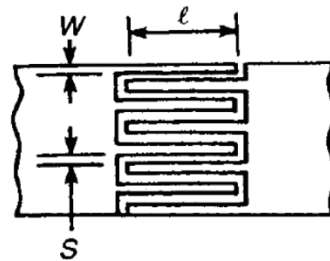

Fig. 5. Layout of the Interdigital Capacitor [34].

To calculate the Interdigital Capacitor values, we use the below equation [5].

$$C(pF) = \frac{\varepsilon_{\varrho} 10^{-3} K(k)}{18\pi K'(k)} (N - 1)l \qquad (1)$$

where:

K(k): is the complete elliptic integral of the first kind

K: Complementary Function of K

$$k = \tan^2\left(\frac{a\pi}{4b}\right)$$

$$a = W/2$$

$$b = (w + s)/2$$

213

$$K' = \sqrt{1 - K^2}$$

$$\varepsilon_e = \begin{cases} \frac{\varepsilon_r+1}{2} + \frac{\varepsilon_r-1}{2}\left[\frac{1}{\sqrt{1+\frac{12h}{w}}} + 0.04\left(1-\frac{w}{h}\right)^2\right] & \text{for } \frac{w}{h} < 1 \\ \frac{\varepsilon_r+1}{2} + \frac{\varepsilon_r-1}{2}\left(\frac{1}{\sqrt{1+\frac{12h}{w}}}\right) & \text{for } \frac{w}{h} > 1 \end{cases}$$
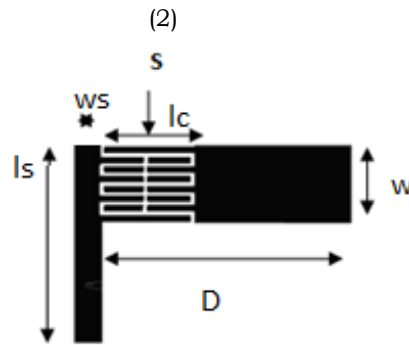
(2)

Fig. 6. Proposed unit cell of the microstrip CRLH TL.

1. Choose center frequency, fo, which represents broadside radiation. (fo=28 GHz)
2. Calculate width required to obtain Zo, set w to this value. (w=5.0 mm).
3. Set stub width, ws, to 20% of w. (ws=1.0 mm).
4. Set stub length (ls=li- w) to w; the electrical length of the stub has to be less than $\Lambda/2$.
5. Set the number of fingers, N, to 6 or 10. Then determine required wc and S=2wc/3. N=6 chosen.

$$w_c \simeq \frac{w}{\frac{5N}{3} - \frac{2}{3}} \simeq 0.39\text{mm}$$

$$S = 0.26\text{mm}$$

6. Calculate length of interdigital finger.

$$l_c \simeq \frac{\Lambda_g}{8} \simeq \frac{c_0}{8f_0\sqrt{\varepsilon_r}} \simeq 8.15\text{mm}$$

After optimization, the geometric parameters are carefully modified. Antenna's actual dimensions are 2.45 mm x 8.21 mm. The final dimensions are displayed in Figure (7) following simulation and optimization using HFFS Software.
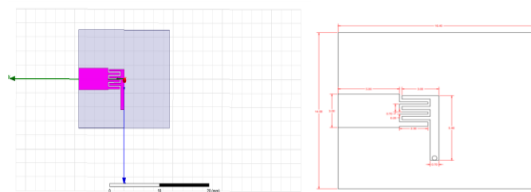

Fig. 7. Geometry Structure of proposed CRLH Antenna in (mm).

The outcomes for the solitary antenna. To verify the simulated outcomes produced by the HFSS software

a- Antenna Return Loss

The suggested 28 GHz antenna's return loss in dB is illustrated in Figure (8). The simulated return loss (reflection coefficient) of the CRLH antenna demonstrates that it can operate (under -10 dB) with a 28 GHz center frequency and a -17.8999 dB bandwidth (FBW16.79%). This indicates that the antenna uses the 5G band.
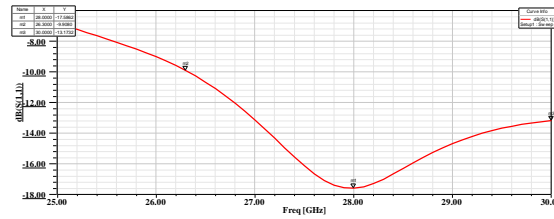
.

Fig. 8. The reflection coefficient of CRLH antenna.

b- Voltage Standing Wave Ratio VSWR

Figure (9) displays the planned single antenna's VSWR. At 28 GHz, we found 1.3 dB with excellent values, indicating good received signals.
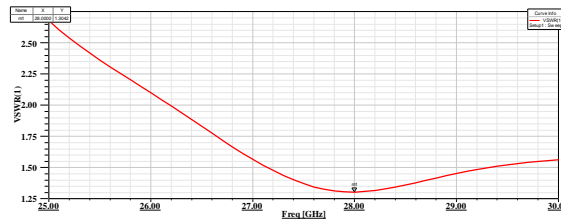

Fig. 9. VSWR of 28 GHz CRLH single antenna.

c- Radiation Pattern

The proposed antenna's simulated 2D and 3D, xz-plane and yz-plane radiation patterns are shown in Figure 10 for the 28 GHz frequency. The developed antenna exhibits good broadside radiation patterns in the xz-plane and yz-plane, as illustrated in Figure (10). The intended antenna emits energy in a focused beam.
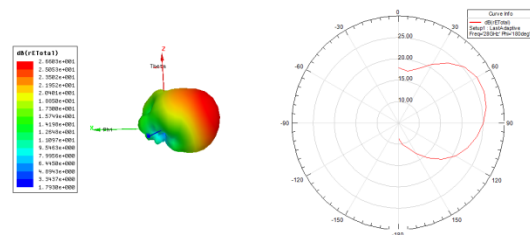

Fig. 10. 2D and 3D radiation pattern of the proposed 28 GHz CRLH antenna .

d- Gain and Directivity

With a gain of 9.149 dB and a directivity of 9.259 dB, the proposed antenna emits a directed beam of radiation. Figure(11) below shows 3D far field plots for gain and directivity. Because of the antenna's strong gain and directivity, its efficiency is 98.8%.
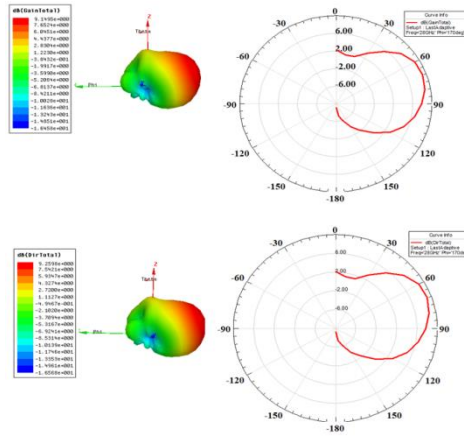
Fig. 11. Gain and directivity of 28 GH the antenna.

f- Current Distribution on the CRLH single antenna

The field distribution between the patch and the ground plane is referred to as the current distribution, and it is utilized as a gauge for the radiation from microstrip patches. The red arrows in Figure (12), which depicts the current distribution pattern at 28 GHz, indicate the strongest current spread in the antenna patch.
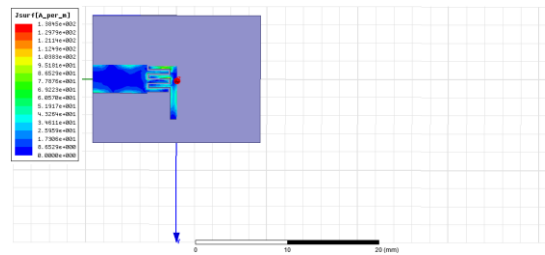

Fig. 12. Current distribution of the CRLH antenna.

From the CRLH single antenna findings (proposed antenna), it can be shown that the antenna performs well at 28 GHz, has a high gain and a directed beam, and is less in size than a typical microstrip antenna—by more than 40%.The multi-port MIMO antenna design for 5G smartphones works well and is suited for this size.

3. **Design of a Metamaterial Multi Port MIMO Antenna (28 GHz)**

Figure (13), which depicts the suggested MIMO antenna's construction. By emphasizing the arrangement of components in an orthogonally symmetric way with various inter-element spacings, the four-port MIMO design development is primarily accomplished. The dimensions of the MIMO antenna are 37371.6 mm3 for a 0 mm edge-to-edge separation (d) between the components. Each MIMO antenna component on the opposing sides of substrate, They make up a structural block and are generally used in 6.5-inch smartphones. They are positioned at one of the four corners of the RT-Duroid 5880 dielectric substrate (loss angle tangent: 0.02, relative permittivity: 2.2). Because the feed line (orange) and ground (blue) are made by printing copper on the front and back of the substrate, it is sometimes referred to as a printed circuit board (PCB). We included an interdigital to lower the mutual coupling and return loss. It should be emphasized that every antenna component is symmetrical in every way. Contrary to the structure used in earlier investigations, which had a CRLH metamaterial TL etched on the dielectric substrate's front surface, the feeding technique results in a

dual-polarized radiation characteristic. The prototype of the suggested antenna is simulated and optimized using HFFS Software to validate this simulation. Each antenna component is made to function in the 28 GHz range. One of the most promising bands for 5G communication is this one. Modern Smartphone devices may make advantage of the MIMO antenna that is being suggested.

An antenna's final performance is optimized by carefully adjusting the geometric characteristics. Antenna's physical dimensions are 76x169x1.6 mm3. Figures (13), and Figure (14), which display the final dimensions following simulation and optimization using HFFS Software.
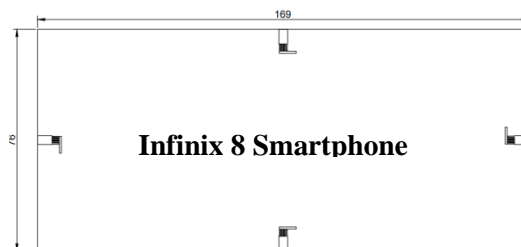

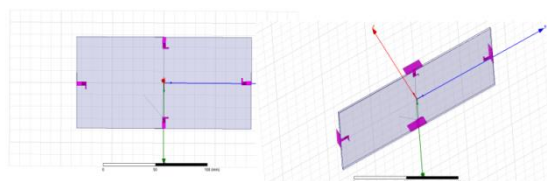**Fig. 13. Layout of the multi port MIMO antenna of CRLH MIMO antenna.**

Fig. 14. Geometry structure of proposed MIMO antennas.

In HFSS, the published structure is implemented. To acquire the scattering parameters, the required simulations are run. The collected findings lined up with the data that had been published, completing the antenna validation. The outcomes for the solitary antenna. in order to verify the computer-simulated outcomes produced by HFSS software.

a- Antenna Return Loss (reflection coefficient) and mutual coupling

Figure (15) shows that the return loss values for S11, S22, S33, and S44 have reached the target value of less than -10 dB, which is centered at 28 GHz with -12.76, -12.5, -12.4, and -12.33 dB, bandwidth that ranges from 2.05 GHz to 2.2 GHz, indicating that the antenna is operating at 5G band.
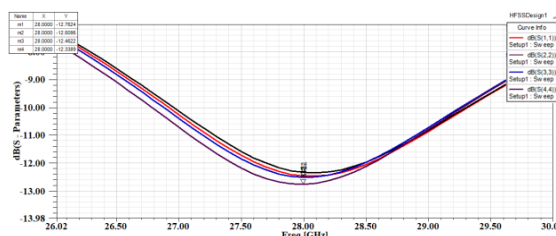

Fig. 15. The Reflection coefficient (S11S22, S33, and S44) of the 4-Port 28 GHz MIMO antenna.

However, the corresponding observed isolation parameter values for S12, S13, S14 and S41, S42, S43,... etc ranged from -44.5 dB to 51 dB at the 28 GHz resonance frequency, as shown in Figure (16). The minimum isolation between the ports in the simulated frequency range is more than -51 dB. The

manufacturing mistake and port/cable coupling losses that caused the difference in these data indicate that high isolation was achieved.
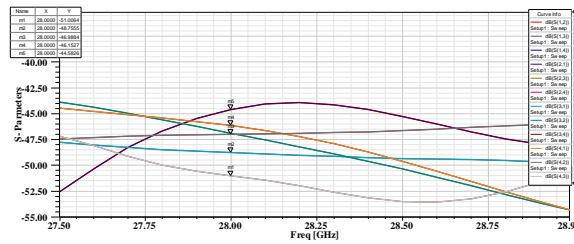

Fig. 16. The Mutual Coupling (S12, S13, and S14) and (S41, S42, and S43) (S21, S23, and S24) and (S31, S32, and S34) of 4-Port 28 GHz MIMO antenna.

b- Voltage Standing Wave Ratio (VSWR)

The measured isolation parameters VSWR-1, VSWR-2, VSWR-3, and VSWR-4 at 28 GHz resonant frequency match to the values of 1.59, 1.62, 1.62, and 1.63 in Figure (17), which depicts the VSWR for 4G-LTE MIMO antenna. This indicates well received signals when the values are good.
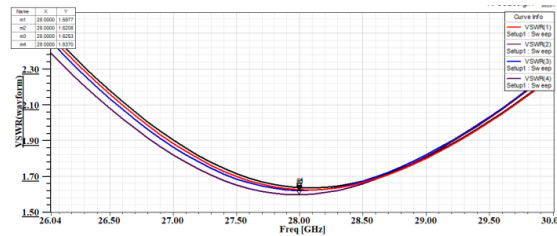

Fig. 17. VSWR (1,2,3,4) of the Proposed MIMO Antenna.

c- Radiation Pattern Gain and Directivity of the Proposed MIMO Antenna

Antenna 1 is terminated with 50 impedances, while the other three elements are produced with far-field patterns in an anechoic room. Due to the proposed antenna's symmetry, port 1 is measured because other ports produce the same patterns when activated. Figure (18) depicts the radiation patterns for the proposed MIMO antenna for the 5G frequency. Since the antennas are patch type, the radiation patterns in the phi=0 deg (x-y plane) and phi=90 deg (y-z plane) planes are directional as would be expected.
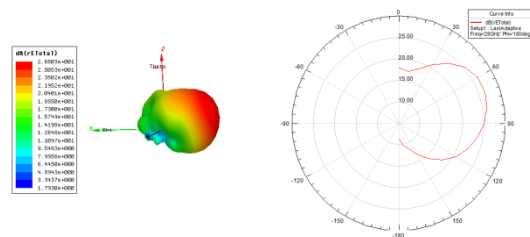

Fig. 18. 2D and3D Radiation Pattern of the Proposed MIMO Antenna.

For Ant.1, Ant.2, Ant.3, Ant.4, the suggested design shows a simulated peak gain value of 9.149 dB and the directivity of 9.259 dB. The antenna efficiency is around 81%. Figure (19) below shows the 2D and 3D far field plots for the planned antenna's gain and directivity. The antenna's gain and directivity are also good.
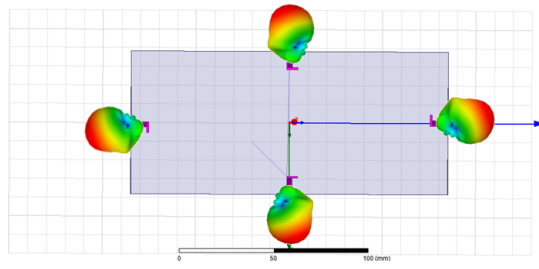
Fig. 19. Gain and Directivity of the proposed 28 GHz MIMO antenna .

d- Current Distribution and E-field on the proposed MIMO Antenna

Investigating the surface current density allowed for a deeper analysis of the reported MIMO antenna system's radiating process. Investigating the antenna components that affect radiation characteristics and clarifying the degree of connection between various MIMO antennas were the main goals of this study. When port 1 is enabled at 28 GHz, the surface current distribution is shown in Figure (20). The feed line and the margins of the slot-shaped antenna are where the current is most heavily concentrated. Additionally, the ground's rectangular holes show a noticeable current dispersion. The metamaterial in radiation behavior is established by this. Additionally, as seen in Figure 20, the metamaterial makes the concentration of the coupling current between MIMO antennas minimal.
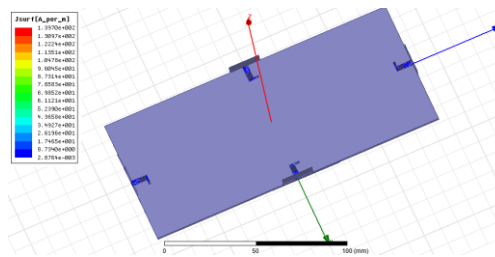

Fig. 20. Current distribution on the proposed 28 GHz MIMO Antenna.

4. **MIMO Performance Parameters The parameters, which have been studied to analyze the performance of MIMO antennas include.**

1- Envelope Correlation Coefficient 'ρ' (ECC)

The degree of coupling between various antenna components in a MIMO system is measured using the envelope correlation coefficient (). The performance of the decoupling increases with decreasing envelope correlation coefficient value. Ideally, it is 0, but in reality it is less than 0.5. Higher isolation results from a lower ECC value, which improves diversity performance. In [5], formula expresses the S parameters based on the suggested four-port MIMO antenna's calculated ECC of 0.3.

2- Total active reflection coefficient (TARC)

One of the diversity parameters used to verify the accuracy of the observed S parameters is the TARC. Random signals and their phase angles for adjacent and diagonal ports are involved. Additionally, for specific phase angles between ports, it confirms the true behavior of the isolation parameters S12, S13, and S14. Efficiency and bandwidth will be impacted when all antenna components are used in MIMO at once. Therefore, the TARC is a reliable tool for determining the MIMO system's performance

over S parameters. When the first port is kept constant while the input signals of the other three ports are stimulated with phase variations between 0 and 180, TARC is monitored. According to calculations, TARC is 27 dB for 28 GHz. This guarantees steady TARC and shows little mutual coupling between the ports.

3- Diversity Gain (DG)

For the MIMO arrangement, diversity gain illustrates "the loss in transmission power when diversity schemes are performed on the module." included in source [5]. According to calculations, the DG is around 9.2 dB across the band, which guarantees that the antenna will perform well in terms of diversity.

4- Channel Capacity Loss (CLL)

The number of radiators in a MIMO system enhances the channel capacity without increasing bandwidth or transmitted power levels. However, interference between the components reduces capacity. CCL can only go as fast as 0.4 bits/s/Hz. CCL was added to the list of MIMO performance characteristics, giving information on the system's channel capacity losses due to the correlation effect. Equations from [5] are used to quantitatively compute the CCL. Calculation shows that the obtained CCL for the proposed MIMO antenna is less than the realistic requirement of 0.4 bit/s/Hz over the entire 28 GHz operating spectrum, ensuring the proposed system's high throughput.

5. Conclusion

This work introduces a unit cell antenna based on metamaterials methods. First, a discussion and design for a single antenna have been made. It has been claimed that good optimization, good matching, and a typical radiation pattern across the antenna MIMO. The findings support a good compromise between the radiation pattern and reflection coefficient that generated a frequency range with good matching properties starting at around 28 GHz. The minimum value of VSWR is around 1.3 at 28 GHz, and the bandwidth ranges from 26.3 GHz to 31 GHz (FBW16.79%). The reflection coefficient S11 is -17.8999 dB. The suggested MIMO antenna has a directedness of 9.25 dB and a gain of 9.14 dB, indicating strong reception signal and a directional beam radiation pattern. The suggested antenna's benefits include compactness (8x3x1.6 mm3 in dimension, a size decrease of about 60%). Additionally, it is pretty obvious that the suggested antenna operating band complies with the 5G standard operating frequency design criteria.

The primary goal of the study is to propose and analyze a 4-port MIMO antenna for 5G smartphone designs with good isolation. The suggested shaped construction produced high isolation performance. Four antennas make up the construction of the proposed MIMO antenna. Each of the four corners of the RT-Duroid 5880 dielectric substrate (relative permittivity=2.2, antenna elements on opposing sides form a structural block) is occupied by an antenna element. loss angle tangent is 0.02). The substrate has a 1.6 mm and is commonly utilized in the Infinix 8 Smartphone. the gain is 9.25 dB, the directivity is 9.14 dB, and the reflection coefficient S11 is -12.76 dB, which indicates a good reception signal and directed radiation pattern for each port. Metamaterials are used to enhance gain and directivity. The advantages of the suggested antenna include compactness, which results in a size reduction of about 60%. Additionally, the developed antenna provides improved values for the observed isolation parameters S12, S13, and S14 between the two ports at operating frequencies, ranging from -44.5 dB to 51 dB at 5.06 GHz resonant frequency. Without the use of any additional structure such as DGS or

parasitic elements, the orientation of the interdigital capacitor has reduced the mutual coupling between two antennas, demonstrating the effectiveness of metamaterials in reducing the electric field distributed between antennas. The concentration of the coupling current between MIMO antennas is negligible as a result of the metamaterials' structural design. Additionally, the proposed system's high throughput is guaranteed by the MIMO performance metrics, which include the envelope correlation coefficient (ECC) of 0.3, diversity gain (DG) of 0.92 dB, total active reflection coefficient (TARC) of -27, and channel capacity loss (CCL) of less than 0.4 bit/s/Hz. The suggested antennas are simple and inexpensively fabricatable. Utilizing a substrate material with a low dielectric constant, the suggested antenna is small and thin. All simulations in this study have been carried out using the electromagnetic program Ansoft HFSS, making it clearly evident that these properties of the proposed antenna operating at 28 GHz band fulfill the design criteria of 5G standard operating frequency.

References

E, Ezhilarasan. And M. Dinakaran,"A Review on Mobile Technologies: 3G, 4G and 5G,", 2nd International Conference on Recent Trends and Challenges in Computational Models, India, February 2017Primer "Wi-Fi: Overview of the 802.11 Physical Layer and Transmitter Measurements", Copyright © 2013,

M. Jensen,"A history of MIMO wireless communications,". In Proceedings of the 2016 IEEE International Symposium on Antennas and Propagation, July 2016.

V. Viktor, "The electrodynamics of substances with simultaneously negative values of and μ.", Soviet Physics, 2016.

M. Alibakhshikenar, "A Comprehensive Survey of "Metamaterial Transmission-Line Based Antennas: Design, Challenges, and Applications", IEEE ACCESS.2020.

C. Caloz and T. Itoh, "Electromagnetic Metamaterials: Transmission Line Theory and Microwave Applications". New York: Wiley, 2004.